

Estimation of 3D rotation for a satellite from Sun sensors

L. Magnis* N. Petit*

* *MINES ParisTech, CAS, 60 bd Saint-Michel, 75272 Paris Cedex
FRANCE (e-mail: lionel.magnis@mines-paristech.fr)*

Abstract: This paper exposes a method to estimate the rotation of a satellite by means of simple Sun sensors located on its surface. It is shown that a minimal setup of 4 sensors is sufficient to estimate the 3D rotation of the rigid body under some mild assumptions bearing on the inertia parameters of the body and the direction of the Sun. The method is a 3D generalization of an approach originally proposed, using the same setup of sensors, for a rotation restricted to take place about a single axis. Taking into consideration the 3D rotation, the estimation problem is geometrically recast into a simple sources separation problem for the measurement equation. This problem is shown to be feasible through a careful investigation of the free motion dynamics using Jacobi elliptic functions which guarantees sufficient frequency difference between the sources.

Keywords: Attitude estimation. Vector measurement. Free-rotation. Frequency analysis.

1. INTRODUCTION

This paper generalizes a recently introduced method to reconstruct the rotation of a rigid body using cheap illumination sensors mounted on its surface (Magnis and Petit [2013]). Originally, this method was limited to cases of rotation about a constant axis, so that the problem could be formulated in 2D. The scope of applicability of this method, which can be considered as an alternative to several well established estimation principles, is here extended to cases of nonzero nutations (tilting of the axis).

In its simplest form, the problem under consideration can be exemplified as follows. Consider a satellite orbiting around the Earth, one desires to estimate the attitude of from Sun sensors. This is a classic question for aerospace applications (see Bruninga [2007]). Typically envisioned cases of application range from deployment of micro-satellite from the ISS (International Space Station) to attitude monitoring of spin or dual-spin satellite and early detection and diagnosis of attitude instability. While several estimation techniques have been considered earlier, including video processing, inertial navigation, magnetometry attitude determination (see e.g. Bak [1999]), it is generally considered that the data produced with these techniques have to be consolidated using another source of information. Sun sensors, which are commonly available (Hall and Harris [1970]), seem like a promising solution. Indeed, these sensors are considered as dependable and using them does not require any further investments.

To employ Sun sensors for estimating rotations, one has to understand their functioning. The energy deposited in a photocell being proportional to the cosine of the angle of incidence of solar radiation, the output signal of a Sun sensor is, roughly speaking, a cosine function of this angle. Thus, using several sensors distributed onto the rigid body, one can obtain an estimation of the Sun vector expressed

in a body frame. This property can be used to estimate the planar rotation of a satellite with four Sun sensors alone (Magnis and Petit [2013]). To generalize this approach to the case of a 3D rotation, we employ the same setup of sensors. Actually, investigations conducted in this article show that a full 3D rotation motion can be estimated.

The set of sensors generate a signal which is impacted by the nutation, the precession and the spin. In this paper, we establish conditions guaranteeing that this impact can be exploited to estimate the full attitude of the rigid body under consideration.

The outcome of this article can seem surprising at first, as it is generally considered that one vector measurement is not enough to determine a 3D orientation (this fact is formulated in the classic Wahba's problem, see Wahba [1965], Choukroun et al. [2006]). From this viewpoint, Sun sensors are often used in combination with another vector measurement device, such as a magnetometer for low earth-orbit (Theil et al. [2003], Schimdt et al. [2008]). However, this paper deals with another way of exploiting Sun vector measurements. As we will show it in this contribution, the spectral content of the Sun sensor measurement generated by the rotation motion has the potential to allow one to recover several interesting informations on the 3D rotation. This is particularly true in free-motion, i.e. when no torques are exerted on the rigid body.

The paper is organized as follows. In Section 2 we introduce notations and define the rotation estimation problem. Introducing a convenient representation of the rotation by means of Euler angles, we compute the measurement equation (i.e. the signal produced by the Sun sensors during the body rotation). The obtained formula contains several terms where the role of each Euler angle is highlighted. In Section 3, we analyze the spectral content of the measurements. We show that, provided the various factors of the

measurement equation satisfy some frequency separation properties, one can separately estimate the angles. From this simple data analysis, the nature of the error is detailed. In Section 4, we invoke the theory of free-motion and use it to establish analytic formulas involving Jacobian elliptic functions describing the angles histories. These formulas can be used to establish sufficient conditions guaranteeing that the frequency separation properties are satisfied. These conditions bear on the moments of inertia of the rigid body, its initial nutation and its angular momentum. In Section 5 we propose simulation results. They stress the relevance of the method, and illustrate typical estimation errors on the various components of the rotation estimate. Finally, in Section 6 we give perspectives for future works.

2. NOTATIONS AND PROBLEM STATEMENT

We consider a satellite equipped with four Sun sensors pointing coplanar pairwise orthogonal directions

$$n_1, n_2, n_3 = -n_1, n_4 = -n_2$$

as shown in Figure 1. Note $I_1 \geq I_2 > I_3$ the inertial moments of the satellite. We consider two frames of reference: the body-attached frame

$$(n_1, n_2, n_1 \times n_2)$$

and an inertial frame (e_1, e_2, e_3) .

With such a sensor setup, at all times exactly two sensors produce a nonzero signal generated by the perceived sunlight represented by the vector S , the other two sensors being in the shadow of the satellite. The (normalized) output signal of sensor i is:

$$y_i = \max(S \cdot n_i, 0)$$

where S is the unit vector pointing the direction of the Sun and \cdot designates the scalar product. As $n_3 = -n_1$ and $n_4 = -n_2$, we have

$$y_1 - y_3 = S \cdot n_1 \quad , \quad y_2 - y_4 = S \cdot n_2$$

Note R the rotation between the body frame and the inertial frame. By definition

$$n_1 = Re_1 \quad , \quad n_2 = Re_2 \quad , \quad n_1 \times n_2 = Re_3$$

Thus,

$$y_1 - y_3 = S \cdot Re_1 \quad , \quad y_2 - y_4 = S \cdot Re_2$$

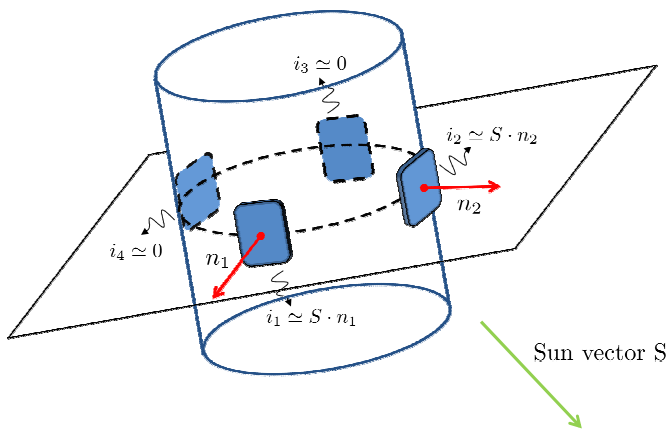


Fig. 1. Satellite equipped with 4 Sun sensors

Gathering the measurements in a complex number, we define

$$y \triangleq y_1 - y_3 + i(y_2 - y_4) = S \cdot (Re_1 + iRe_2) \quad (2.1)$$

Introduce φ, θ, ψ the ZXZ Euler angles of R as in Landau and Lifchitz [1982]. The rotation matrix writes

$$R = \begin{pmatrix} c\varphi c\psi - s\varphi s\psi c\theta & -c\varphi s\psi - s\varphi c\psi c\theta & s\varphi s\theta \\ s\varphi c\psi + c\varphi s\psi c\theta & -s\varphi s\psi + c\varphi c\psi c\theta & -c\varphi s\theta \\ s\psi s\theta & c\psi s\theta & c\theta \end{pmatrix}$$

where

- $\varphi \in [0, 2\pi)$ is the precession angle
- $\theta \in (0, \pi)$ is the nutation angle
- $\psi \in [0, 2\pi)$ is the spin angle
- c,s designate cos, sin respectively

Note (s_1, s_2, s_3) the (constant) coordinates of the Sun vector in the inertial frame. The following result holds

Proposition 1. The coplanar Sun sensors generate a complex-valued measurement y of the form

$$y = \frac{s_1 + is_2}{2}(1 + \cos\theta)e^{-i(\varphi+\psi)} + is_3 \sin\theta e^{-i\psi} + \frac{s_1 - is_2}{2}(1 - \cos\theta)e^{i(\varphi-\psi)} \quad (2.2)$$

Proof According to the expression of R , we have

$$\begin{aligned} y &= s_1 (c\varphi c\psi - s\varphi s\psi c\theta - i(c\varphi s\psi + s\varphi c\psi c\theta)) \\ &\quad + s_2 (s\varphi c\psi + c\varphi s\psi c\theta + i(-s\varphi s\psi + c\varphi c\psi c\theta)) \\ &\quad + s_3 (s\psi s\theta + ic\psi s\theta) \\ &= s_1 (c(\varphi + \psi) - is(\varphi + \psi) + (1 - c\theta)(s\varphi s\psi + is\varphi c\psi)) \\ &\quad + s_2 (s(\varphi + \psi) + ic(\varphi + \psi) - (1 - c\theta)(c\varphi s\psi + ic\varphi c\psi)) \\ &\quad + is_3 s\theta (c\psi - is\psi) \\ &= s_1 e^{-i(\varphi+\psi)} + is_1 (1 - c\theta)s\varphi e^{-i\psi} \\ &\quad + is_2 e^{-i(\varphi+\psi)} - is_2 (1 - c\theta)c\varphi e^{-i\psi} + is_3 s\theta e^{-i\psi} \\ &= (s_1 + is_2)e^{-i(\varphi+\psi)} \\ &\quad + \frac{1 - c\theta}{2} e^{-i\psi} (s_1 e^{i\varphi} - s_1 e^{-i\varphi} - is_2 e^{i\varphi} - is_2 e^{-i\varphi}) \\ &\quad + is_3 s\theta e^{-i\psi} \end{aligned}$$

which gives the conclusion.

Mathematically, we can now formulate our estimation problem as follows

Problem 1. (rotation estimation from Sun sensors).

From measurements of the form (2.2) where φ, ψ, θ are the respective precession, spin and nutation angle of a rigid body and s_1, s_2, s_3 are known constant values, find estimates $\hat{\varphi}, \hat{\psi}, \hat{\theta}$ of the Euler angles.

Remark 1. One can make several choices to define the inertial frame of reference, depending on the analysis one wishes to perform. For example, one can exhibit the non-observability of the rotation angle around the Sun vector as follows. If the inertial frame was chosen so that the Sun vector is aligned with e_3 , then $s_1 = s_2 = 0, s_3 = 1$. The measurement equation (2.2) would reduce to $y = i \sin\theta e^{-i\psi}$. Under this form, it is clear that angles ψ and θ are observable and that φ is not, as it does not impact the measurement. Thus, Problem 1 does not have a satisfying solution in the general case. Typically, troubles will arise if the rigid body is animated

with precession around the Sun vector. In Section 4 we will make a different choice, handy for free-rotation analysis.

In the following, we invoke arguments of frequency separation in signal processing to explain how the sought-after information on the angles can be obtained from the measurements, under careful assumptions.

3. FREQUENCY ANALYSIS OF THE MEASUREMENT EQUATION

We rewrite the measurement equation (2.2) as

$$y(t) = a_1(t) e^{i\phi_1(t)} + a_2(t) e^{i\phi_2(t)} + a_3(t) e^{i\phi_3(t)} \quad (3.1)$$

with

$$\begin{aligned} \phi_1 &\triangleq -\varphi - \psi & a_1 &\triangleq (s_1 + is_2) \frac{1 + \cos \theta}{2} \\ \phi_2 &\triangleq -\psi & a_2 &\triangleq is_3 \sin \theta \\ \phi_3 &\triangleq \varphi - \psi & a_3 &\triangleq (s_1 - is_2) \frac{1 - \cos \theta}{2} \end{aligned}$$

Under this form, the measurement is the sum of three terms with phase ϕ_i and modulated amplitude a_i . Interestingly, if the ϕ_i, a_i and their derivatives satisfy some desirable properties, one can recover the instantaneous frequencies $\frac{d\phi_i}{dt}$ by mean of windowed Fourier transforms (see Mallat [1998] Chapter 4.4) as we will explain below. This is a solution for this source separation problem.

For clarity of the exposition, we assume

$$\theta \ll \frac{|s_3|}{\sqrt{s_1^2 + s_2^2}}, \quad 1$$

which implies $|a_3| \ll |a_1|, |a_2|$. Thus, we consider measurements of the form

$$y = a_1(t) e^{i\phi_1(t)} + a_2(t) e^{i\phi_2(t)}$$

Though we apparently lose generality, one should bear in mind that the following analysis could, with additional tedious but relatively easy calculations, extend to the general case (3.1) (practical implementation remains simple).

Let g be a window function (even, positive, with finite support in $[-0.5, 0.5]$ and unit L_2 norm)

$$\int_{-1/2}^{1/2} g^2(t) dt = 1$$

By definition, its Fourier transform \mathcal{G} satisfies

$$\mathcal{G}(0) \geq \mathcal{G}(\nu), \quad \forall \nu$$

and decays rapidly to 0 when ν grows. This decay is characterized by (among other) the bandwidth $\Delta\nu$ defined as

$$|\mathcal{G}(\frac{\Delta\nu}{2})| = \frac{|\mathcal{G}(0)|}{\sqrt{2}}$$

In general, we have

$$\mathcal{G}(\nu) \ll \mathcal{G}(0), \quad \forall |\nu| \geq 2\Delta\nu$$

Take a scaling factor $\tau > 0$ and define the windowed Fourier transform (a.k.a. spectrogram Mallat [1998]) of the signal y at time u and frequency ξ using g as window scaled by τ as

$$\begin{aligned} S_y(u, \xi) &= \frac{1}{\tau} \int_{-\tau/2}^{\tau/2} y(u+t) g\left(\frac{t}{\tau}\right) e^{-i\xi(u+t)} dt \\ &= \frac{1}{\tau} \int_{-\tau/2}^{\tau/2} a_1(u+t) g\left(\frac{t}{\tau}\right) e^{i[\phi_1(u+t) - \xi(u+t)]} dt \\ &\quad + \frac{1}{\tau} \int_{-\tau/2}^{\tau/2} a_2(u+t) g\left(\frac{t}{\tau}\right) e^{i[\phi_2(u+t) - \xi(u+t)]} dt \\ &\triangleq S_1(u, \xi) + S_2(u, \xi) \end{aligned}$$

The spectrogram satisfies the following property (adapted from Mallat [1998], theorem 4.5).

Proposition 2. For $j = 1, 2$ we have

$$S_j(u, \xi) = a_j(u) e^{i(\phi_j(u) - \xi u)} \mathcal{G}\left(\tau(\xi - \dot{\phi}_j(u))\right) + \varepsilon_j(u, \xi)$$

with

$$|\varepsilon_j(u, \xi)| \leq \frac{\tau}{2\sqrt{3}} |\dot{a}_j(u)| + \frac{\tau^2}{8\sqrt{5}} |\ddot{a}_j|_u + |a_j(u)| \frac{\tau^2}{8\sqrt{5}} |\ddot{\phi}_j|_u \quad (3.2)$$

where $|\cdot|_u$ designates the supremum over $[u - \tau/2, u + \tau/2]$

Before proving this result, let us interpret it. Assuming the error terms ε_j are small, the spectrogram reduces to two main terms

$$\begin{aligned} S_y(u, \xi) &\simeq a_1(u) e^{i(\phi_1(u) - \xi u)} \mathcal{G}\left(\tau(\xi - \dot{\phi}_1(u))\right) \\ &\quad + a_2(u) e^{i(\phi_2(u) - \xi u)} \mathcal{G}\left(\tau(\xi - \dot{\phi}_2(u))\right) \end{aligned}$$

Thus, if the instantaneous frequencies are separated enough with respect to the bandwidth of \mathcal{G} , namely if they satisfy

$$\tau|\dot{\phi}_1 - \dot{\phi}_2| \geq 2\Delta\nu \quad (3.3)$$

then $|S(u, \cdot)|$ has two main lobes for

$$\xi_j \triangleq \dot{\phi}_j(u), \quad j = 1, 2$$

More precisely, we have

$$S_y(u, \dot{\phi}_j(u)) \simeq a_j(u) e^{i[\phi_j(u) - u\dot{\phi}_j(u)]} \mathcal{G}(0)$$

Hence, one can recover the instantaneous frequencies $\dot{\phi}_j(u)$ by detecting the peaks of the spectrogram. Further, the corresponding amplitude of the lobe gives us $a_j(u)$. As will appear, these informations are instrumental in estimating the three Euler angles.

Proof of Proposition 2. For a fixed value (u, ξ) and $t \in [u - \frac{\tau}{2}, u + \frac{\tau}{2}]$, note

$$\begin{aligned} a_j(u+t) &= a_j(u) + t\dot{a}_j(u) + \frac{t^2}{2}\alpha_j(t) \\ \phi_j(u+t) &= \phi_j(u) + t\dot{\phi}_j(u) + \frac{t^2}{2}\beta_j(t) \end{aligned}$$

with

$$|\alpha_j(t)| \leq |\ddot{a}_j|_u, \quad |\beta_j(t)| \leq |\ddot{\phi}_j|_u$$

For brevity, we omit the bounds $\pm \frac{\tau}{2}$ of the integrals below. For $j = 1, 2$ we have

$$\begin{aligned}
 S_j(u, \xi) &= a_j(u) \frac{e^{i[\phi_j(u) - \xi u]}}{\tau} \int g\left(\frac{t}{\tau}\right) e^{-it(\xi - \dot{\phi}_j(u))} dt \\
 &+ a_j(u) \frac{e^{i[\phi_j(u) - \xi u]}}{\tau} \int g\left(\frac{t}{\tau}\right) e^{-it(\xi - \dot{\phi}_j(u))} (e^{i\frac{t^2}{2}\beta_j(t)} - 1) dt \\
 &+ \dot{a}_j(u) \frac{1}{\tau} \int t g\left(\frac{t}{\tau}\right) e^{i[\phi_j(u+t) - \xi(u+t)]} dt \\
 &+ \frac{1}{2\tau} \int t^2 \alpha_j(t) g\left(\frac{t}{\tau}\right) e^{i[\phi_j(u+t) - \xi(u+t)]} dt \\
 &= a_j(u) e^{i[\phi_j(u) - \xi u]} \mathcal{G}\left(\tau(\xi - \dot{\phi}_j(u))\right) + \varepsilon_j(u, \xi)
 \end{aligned}$$

where

$$\begin{aligned}
 |\varepsilon_j(u, \xi)| &\leq |a_j(u)| \int g\left(\frac{t}{\tau}\right) |e^{i\frac{t^2}{2}\beta_j(t)} - 1| \frac{dt}{\tau} \\
 &+ |\dot{a}_j(u)| \int |t| g\left(\frac{t}{\tau}\right) \frac{dt}{\tau} \\
 &+ \frac{|\ddot{a}_j|_u}{2} \int t^2 g\left(\frac{t}{\tau}\right) \frac{dt}{\tau}
 \end{aligned}$$

To conclude, we use the following two technical points.

(1) For any $x \in \mathbb{R}$, we have

$$\begin{aligned}
 |e^{ix} - 1|^2 &= (\cos x - 1)^2 + \sin^2 x \\
 &= 2(1 - \cos x) \\
 &= 2 \sum_{n \geq 1} (-1)^{n-1} \frac{x^{2n}}{(2n)!} \leq x^2
 \end{aligned}$$

Thus, for all t

$$|e^{i\frac{t^2}{2}\beta_j(t)} - 1| \leq \frac{t^2}{2} |\beta_j(t)| \leq \frac{t^2}{2} |\ddot{\phi}_j|_u$$

(2) For any $n \in \mathbb{N}$, we have

$$\begin{aligned}
 \int_{-\tau/2}^{\tau/2} |t^n| g\left(\frac{t}{\tau}\right) \frac{dt}{\tau} &= \tau^n \int_{-1/2}^{1/2} |t|^n g(t) dt \\
 &\leq \tau^n \sqrt{\int_{-1/2}^{1/2} t^{2n} dt} \sqrt{\int_{-1/2}^{1/2} g(t)^2 dt} \\
 &= \frac{\tau^n}{2^n \sqrt{2n+1}}
 \end{aligned}$$

Using the latter point for $n = 1, 2$ ends the proof.

If the separating condition (3.3) is met, the decay of \mathcal{G} isolates the contributions of $S_1(u, \dot{\phi}_1(u))$ and $S_2(u, \dot{\phi}_2(u))$ in the frequency domain. To safely consider that the spectrogram peaks detection will give satisfactory result, one should verify that none of the 6 terms of (3.2) for $j = 1, 2$ perturbrates the location of any of the peaks $\xi = \dot{\phi}_1(u), \dot{\phi}_2(u)$. Gathering these requirements, the following set of conditions guarantees reliability of the peaks detection

$$\begin{aligned}
 \tau|\dot{\phi}_1 - \dot{\phi}_2| &\geq 2\Delta\nu \\
 \tau|\dot{a}_j| &\ll 2\sqrt{3}\mathcal{G}(0)|a_j| \\
 \tau^2|\ddot{a}_j|_u &\ll 8\sqrt{5}\mathcal{G}(0)|a_j(u)|, \quad \forall u \\
 \tau^2|\ddot{\phi}_j| &\ll 8\sqrt{5}\mathcal{G}(0)
 \end{aligned}$$

Noting

$$c_1 = 2\sqrt{3}\mathcal{G}(0) \quad , \quad c_2 = 8\sqrt{5}\mathcal{G}(0),$$

converting these conditions in terms of Euler angles yields

$$\left. \begin{aligned}
 \tau|\dot{\phi}| &\geq 2\Delta\nu \\
 \tau|(\cos \theta)'| &\ll c_1(1 + \cos \theta) \\
 \tau|(\sin \theta)'| &\ll c_1|\sin \theta| \\
 \tau^2|(\cos \theta)|_u &\ll c_2(1 + \cos \theta(u)), \quad \forall u \\
 \tau^2|(\sin \theta)|_u &\ll c_2|\sin \theta(u)|, \quad \forall u \\
 \tau^2|\ddot{\psi}|, \tau^2|\ddot{\phi} + \ddot{\psi}| &\ll c_2
 \end{aligned} \right\} \quad (3.4)$$

When g is e.g. a normalized Hann window, we have

$$\Delta\nu \simeq 9.05 \text{ [rad]}, \quad c_1 \simeq 2.83, \quad c_2 \simeq 14.61$$

If the conditions (3.4) are satisfied, then the study of the local maxima (their arguments and value) of Sy will give a convenient and reliable solution to the stated problem. In detail, we use the following algorithm (solution to the stated Problem 1).

Algorithm [under assumptions (3.4)]

Inputs :

- sampled data $y[k]$, sampling time $t[k]$
- window function g
- window size τ

Steps for each $t[k]$

- calculate the spectrogram $Sy(t[k], \cdot)$ (e.g. by mean of a fast Fourier Transform)
- find the two main lobes of $|Sy(t[k], \cdot)|$ corresponding to frequencies ξ_1, ξ_2 with $|\xi_1| > |\xi_2|$ and amplitudes m_1, m_2 (e.g. by an exhaustive search of local maxima)
- compute estimates

$$\widehat{\frac{d\psi}{dt}}[k] = -\xi_2$$

$$\widehat{\frac{d\phi}{dt}}[k] = \xi_2 - \xi_1$$

- estimate $\phi[k], \psi[k]$ by cumulative numerical integration of the estimates of their respective derivative defined above
- estimate $\theta[k]$ from

$$\widehat{\cos \theta}[k] = \frac{2m_1}{\sqrt{s_1^2 + s_2^2} \mathcal{G}(0)} - 1$$

$$\widehat{\sin \theta}[k] = \frac{m_2}{|s_3| \mathcal{G}(0)}$$

Remark 2.

- The algorithm provides average values (over a time window of size τ) of $\dot{\phi}, \dot{\psi}$ and θ . Thus, it does not allow to observe high-frequency variations (compared to $\frac{1}{\tau}$) of these quantities.
- The algorithm needs initial values of ϕ and ψ to estimate the full rotation.
- The computation of $Sy(t[k], \cdot)$ requires the values of y over $[t[k] - \tau/2, t[k] + \tau/2]$.

In the next section, we determine sufficient conditions such that (3.4) hold in the case of a free rotation.

4. ROTATION ANALYSIS IN FREE-MOTION

We consider that the motion of our satellite satisfy the equations of (torque) free-motion. We establish sufficient conditions bearing on the system parameters (inertia)

and the initial condition guaranteeing practicability of the previously described technique of estimation.

We refer to the notations of Landau and Lifchitz [1982] (the following derivation could also be found in a more modern formulation in Abraham and Marsden [1978] or Murray et al. [1994]). Note Ω and \mathbf{M} the angular velocity, respectively angular momentum, of the satellite, and $(\Omega_1, \Omega_2, \Omega_3)$, (M_1, M_2, M_3) their coordinates in the body frame. We have

$$M_i = I_i \Omega_i, \quad i = 1, 2, 3$$

The angular velocity and the Euler angles are related by

$$\Omega_1 = \dot{\varphi} \sin \psi \sin \theta + \dot{\theta} \cos \psi \quad (4.1)$$

$$\Omega_2 = \dot{\varphi} \cos \psi \sin \theta - \dot{\theta} \sin \psi \quad (4.2)$$

$$\Omega_3 = \dot{\varphi} \cos \theta + \dot{\psi}$$

In this section we consider the particular case of a free rotation (i.e: no torque). This assumption implies that \mathbf{M} is constant over time, and that the Ω_i satisfy the free Euler equations

$$I_1 \dot{\Omega}_1 + (I_3 - I_2) \Omega_2 \Omega_3 = 0$$

$$I_2 \dot{\Omega}_2 + (I_1 - I_3) \Omega_3 \Omega_1 = 0$$

$$I_3 \dot{\Omega}_3 + (I_2 - I_1) \Omega_1 \Omega_2 = 0$$

An adequate choice of the inertial frame allows one to compute explicit expression of the Euler angles depending on two parameters only, the norm of the angular momentum $M \triangleq |\mathbf{M}|$ and the initial nutation θ_0 . For clarity, we introduce two scaling parameters, ϵ and λ , as follows

$$I_1 \triangleq I_2(1 + \epsilon)$$

$$I_1 \triangleq I_3(1 + \lambda)$$

ϵ scales the symmetry of the satellite around the I_3 axis ($\epsilon = 0$ correspond to a symmetric satellite), while λ scales the elongation of the satellite along this axis. We have the following equivalence

$$I_1 \geq I_2 > I_3 \Leftrightarrow 0 \leq \epsilon < \lambda$$

4.1 Angular velocities

Conveniently, we choose the inertial frame so that \mathbf{M} is aligned with the vertical vector e_3 . Then, we have

$$I_1 \Omega_1 = M \sin \psi \sin \theta \quad (4.3)$$

$$I_2 \Omega_2 = M \cos \psi \sin \theta \quad (4.4)$$

$$I_3 \Omega_3 = M \cos \theta \quad (4.5)$$

Further, we choose the inertial frame so that

$$\psi(0) = \frac{\pi}{2}, \quad \theta(0) = \theta_0$$

or equivalently

$$\Omega_1(0) = \frac{M}{I_1} \sin \theta_0, \quad \Omega_2(0) = 0, \quad \Omega_3(0) = \frac{M}{I_3} \cos \theta_0$$

The motions under consideration in this study are such that

$$\frac{\epsilon}{\lambda} < \cos^2 \theta_0 < 1 \quad (4.6)$$

This condition will later guarantee that the oscillations of θ have magnitude smaller than $\frac{\pi}{2}$. Note

$$\begin{aligned} \alpha &\triangleq \frac{\epsilon}{\lambda - \epsilon} \\ k &\triangleq \sqrt{\alpha} \tan \theta_0 \\ w &\triangleq \sqrt{\lambda(\lambda - \epsilon)} \frac{M}{I_1} \cos \theta_0 \\ A_1 &\triangleq \frac{M}{I_1} \sin \theta_0 = \Omega_1(0) \\ A_2 &\triangleq (1 + \epsilon) \sqrt{\frac{\lambda}{\lambda - \epsilon}} A_1 \\ A_3 &\triangleq \frac{M}{I_3} \cos \theta_0 = \Omega_3(0) \\ \omega_i &\triangleq \frac{\Omega_i}{A_i}, \quad i = 1, 2, 3 \end{aligned}$$

Condition (4.6) guarantees that $k \in (0, 1)$. The Euler equations become

$$\begin{aligned} \frac{d\omega_1}{d(wt)} &= \omega_2 \omega_3 & \omega_1(0) &= 1 \\ \frac{d\omega_2}{d(wt)} &= -\omega_3 \omega_1 & \omega_2(0) &= 0 \\ \frac{d\omega_3}{d(wt)} &= k^2 \omega_1 \omega_2 & \omega_3(0) &= 1 \end{aligned}$$

Thus, see Abramowitz and Stegun [1964] page 574, $(\omega_1, -\omega_2, \omega_3)$ satisfy the differential equation of the Jacobian elliptic functions $\text{cn}, \text{sn}, \text{dn}$ of parameter k^2 . As a result, we have

$$\begin{aligned} \Omega_1(t) &= A_1 \text{cn}(wt) \\ \Omega_2(t) &= -A_2 \text{sn}(wt) \\ \Omega_3(t) &= A_3 \text{dn}(wt) \end{aligned}$$

Note

$$T = \frac{4}{w} \int_0^1 \frac{dx}{\sqrt{1-x^2} \sqrt{1-k^2x^2}}$$

By construction, Ω_1 and Ω_2 are T -periodic, Ω_3 is $\frac{T}{2}$ -periodic.

4.2 Euler angles

In our problem, the nutation angle is characterized by its cosine value. From (4.5) we have

$$\begin{aligned} \cos \theta(t) &= \frac{I_3}{M} \Omega_3(t) \\ &= \cos \theta_0 \text{dn}(wt) \\ &= \cos \theta_0 \sqrt{1 - k^2 \text{sn}^2(wt)} \end{aligned} \quad (4.7)$$

Thus, we have

$$\begin{aligned} \frac{d}{dt} \cos \theta(t) &= \cos \theta_0 w (\text{dn}(wt))' \\ &= -k^2 w \cos \theta_0 \text{sn}(wt) \text{cn}(wt) \\ \frac{d^2}{dt^2} \cos \theta(t) &= k^2 w^2 \cos \theta_0 \text{dn}(wt) (\text{sn}^2(wt) - \text{cn}^2(wt)) \\ \sin \theta(t) &= \sin \theta_0 \sqrt{1 + \alpha \text{sn}^2(wt)} \\ \frac{d}{dt} \sin \theta(t) &= \alpha \sin \theta_0 \frac{\text{sn}(wt) \text{cn}(wt) \text{dn}(wt)}{\sqrt{1 + \alpha \text{sn}^2(wt)}} w \end{aligned}$$

Hence, using (4.7) and the preceding relations

$$\begin{aligned}\cos \theta &\geq \cos \theta_0 \sqrt{1 - k^2} \\ &= \sqrt{\frac{\lambda \cos^2 \theta_0 - \epsilon}{\lambda - \epsilon}} \\ |(\cos \theta)'| &\leq \epsilon \sqrt{\frac{\lambda}{\lambda - \epsilon}} \frac{\sin^2 \theta_0}{2} \frac{M}{I_1} \\ |(\cos \theta)''| &\leq \epsilon \lambda \sin^2 \theta_0 \cos \theta_0 \left(\frac{M}{I_1}\right)^2 \\ \sin \theta &\geq \sin \theta_0 \\ |(\sin \theta)'| &\leq \frac{\alpha w \sin \theta_0}{2} \\ &= \epsilon \sqrt{\frac{\lambda}{\lambda - \epsilon}} \frac{\sin \theta_0}{2} \frac{M}{I_1} \cos \theta_0 \\ |(\sin \theta)''| &\leq (1 + \alpha) \alpha w^2 \sin \theta_0 \\ &= \frac{\epsilon \lambda^2}{\lambda - \epsilon} \left(\frac{M}{I_1}\right)^2 \cos^2 \theta_0 \sin \theta_0\end{aligned}$$

The spin angle is recovered via the value of its tangent from (4.3),(4.4)

$$\begin{aligned}\tan \psi(t) &= \frac{I_1 \Omega_1(t)}{I_2 \Omega_2(t)} \\ &= -\sqrt{\frac{\lambda - \epsilon \operatorname{cn}(wt)}{\lambda}} \frac{\operatorname{sn}(wt)}{\operatorname{sn}(wt)}\end{aligned}$$

After some calculations, ones has

$$\begin{aligned}\dot{\psi}(t) &= \frac{\lambda(\lambda - \epsilon) \operatorname{dn}(wt)}{\lambda - \epsilon + \epsilon \operatorname{sn}^2(wt)} \frac{M}{I_1} \cos \theta_0 > 0 \\ \ddot{\psi}(t) &= \frac{-\lambda \epsilon (\lambda - \epsilon) \cos \theta_0}{(\lambda - \epsilon + \epsilon \operatorname{sn}^2(wt))^2} \frac{M}{I_1} w \left(\operatorname{dn}^2(t) + \frac{1}{\cos^2 \theta_0} \right)\end{aligned}\quad (4.8)$$

Equations (4.1) and (4.2) give the derivatives of the precession angle

$$\begin{aligned}\dot{\varphi}(t) &= \frac{\Omega_1(t) \sin \psi(t) + \Omega_2(t) \cos \psi(t)}{\sin \theta(t)} \\ &= \frac{I_1 \Omega_1^2(t) + I_2 \Omega_2^2(t)}{I_1^2 \Omega_1^2(t) + I_2^2 \Omega_2^2(t)} M \\ &= \frac{\lambda - \epsilon + (1 + \lambda) \epsilon \operatorname{sn}^2(wt)}{\lambda - \epsilon + \epsilon \operatorname{sn}^2(wt)} \frac{M}{I_1} > 0\end{aligned}\quad (4.9)$$

$$\ddot{\varphi}(t) = \frac{\lambda \epsilon (\lambda - \epsilon)}{(\lambda - \epsilon + \epsilon \operatorname{sn}^2(wt))^2} \frac{M}{I_1} w \times 2 \operatorname{dn}(wt)\quad (4.10)$$

Note that, from (4.7), θ oscillates between θ_0 and $\arccos(\theta_0 \sqrt{1 - k^2}) < \frac{\pi}{2}$, whereas φ and ψ are strictly increasing. From (4.9), (4.10) and (4.8) one has

$$\begin{aligned}\frac{M}{I_1} \leq \dot{\varphi} &\leq \frac{M}{I_1} (1 + \epsilon) \\ |\ddot{\psi}| &\leq \epsilon \lambda \sqrt{\frac{\lambda}{\lambda - \epsilon}} \frac{1 + \cos^2 \theta_0}{2} \left(\frac{M}{I_1}\right)^2 \\ |\ddot{\varphi} + \ddot{\psi}| &\leq \frac{1}{2} \epsilon \lambda \sqrt{\frac{\lambda}{\lambda - \epsilon}} \left(\frac{M}{I_1}\right)^2\end{aligned}$$

4.3 Conditions to guarantee frequency separation

Considering the analytic expressions derived above for the Euler angles and their derivatives, one can formulate conditions bearing only on $\frac{M}{I_1}$, λ , ϵ and the initial nutation θ_0 to guarantee that (3.4) holds.

$$\begin{aligned}\tau \frac{M}{I_1} &\geq 2\Delta\nu \\ \tau \frac{M}{I_1} \epsilon \sqrt{\frac{\lambda}{\lambda - \epsilon}} &\ll 2c_1 \\ \left(\tau \frac{M}{I_1}\right)^2 \epsilon \frac{\lambda^2}{\lambda - \epsilon} &\ll c_2\end{aligned}$$

One can regroup and simplify these conditions in the case of a nearly symmetric satellite, which gives the following result.

Proposition 3. If ϵ satisfies

$$\epsilon \ll \lambda$$

then the following conditions guarantee that (3.4) hold

$$\begin{aligned}\tau \frac{M}{I_1} &\geq 2\Delta\nu \\ \tau \frac{M}{I_1} \epsilon &\ll 2c_1 \\ \left(\tau \frac{M}{I_1}\right)^2 \epsilon \lambda &\ll c_2\end{aligned}$$

Remark 3. These assumptions rule out rotation movements with strong precession around the Sun vector (see Remark 1).

5. SIMULATION RESULTS

For illustration we simulate a satellite as a homogeneous ellipsoid with semi-axes 0.5 m, 0.75 m, 1 m and mass 200 kg. We use parameters

$$\begin{aligned}M &= 1500 \text{ [kg.m}^2\text{/s]} \\ \theta_0 &= 0.3 \text{ [rad]} \\ s_1 = s_2 = s_3 &= \frac{1}{\sqrt{3}}\end{aligned}$$

which gives

$$\begin{aligned}\frac{M}{I_1} &= 6 \text{ [rad/s]} \\ \lambda &= 0.92 \\ \epsilon &= 0.25 \\ \Omega_1(0) &= 1.77 \text{ [rad/s]} \\ \Omega_2(0) &= 0 \\ \Omega_3(0) &= 11.0 \text{ [rad/s]} \\ T &= 1.31 \text{ [s]}\end{aligned}$$

For the windowed Fourier transforms we use

$$\begin{aligned}g(t) &= 2\sqrt{\frac{2}{3}} \cos^2 \pi t \quad (\text{Hann window}) \\ \tau &= 6 \text{ [s]}\end{aligned}$$

The differential equations for the angular velocity and Euler angles were solved using explicit computation of the Jacobian elliptic functions for Ω_i , θ , ψ , $\dot{\varphi}$. The corresponding motion is reported in Figure 2. $\theta(t)$ is $\frac{T}{2}$ periodic. ψ and φ grow in an almost affine fashion, up to a bounded term. This last term (hardly visible in Figure 2) is T -periodic for ψ and aperiodic for φ . Therefore, the satellite never goes back to its initial attitude (see Landau and Lifchitz [1982] page 182).

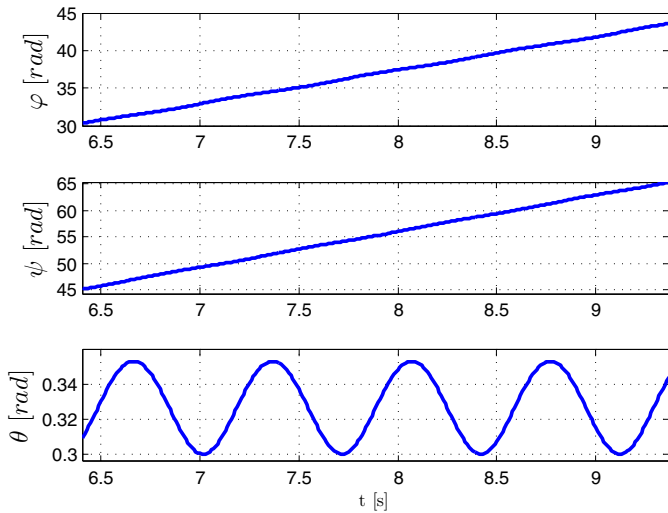


Fig. 2. Euler angles

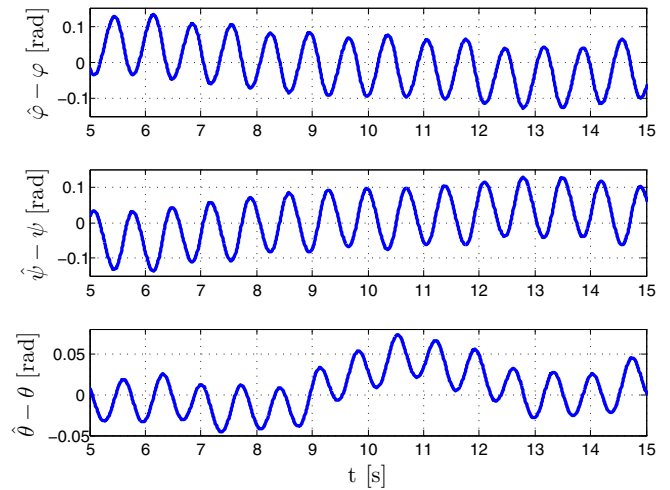


Fig. 4. Euler angles estimation error

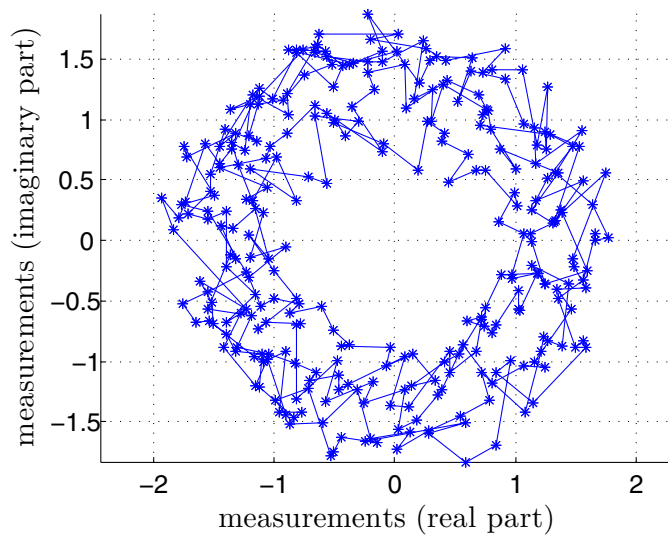


Fig. 3. Measurements corrupted by noise

The considered measurements are of the form (2.1) with complex additive Gaussian white noise of covariance $0.15 \times I_{2 \times 2}$. They are represented in Figure 3.

The estimating errors of the angles are given in Figure 5 over 10 s. Reconstruction of φ and ψ is very satisfactory. The reconstruction error remains bounded at all times while these quantities steadily grow. On the other hand, reconstruction of the (at-all times bounded) nutation is less accurate. The estimator catches the mean value of θ but, as expected (see Remark 2) the oscillations remain undamped. However, this is already satisfactory especially with respect to the relatively little importance of this variable on the problem of estimating the satellite orientation. To confirm this, we report the Frobenius norm of the error of the estimation of the rotation matrix in Figure 5. This absolute error is below 6%. To highlight the importance of the scaling factor τ , we compute the spectrogram $|Sy|$ for the set of parameters of the example with $\tau = 6s$ and for the same set of parameters with a different $\tau = 4s$ in Figures 6 and 7. In both figures, one can clearly see the two main lobes of the spectrogram and

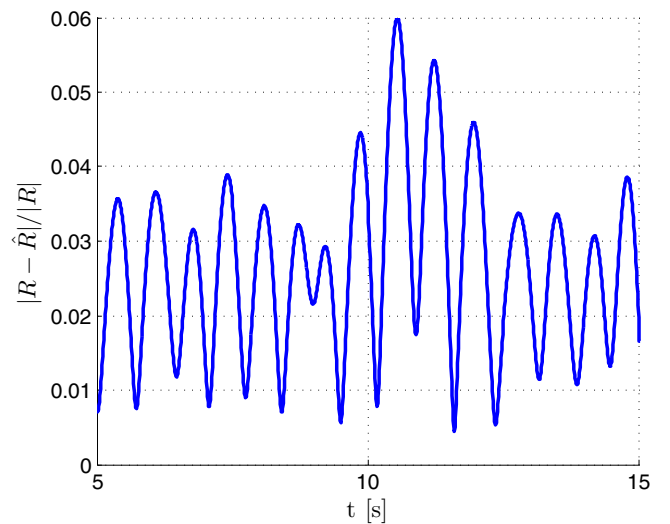


Fig. 5. Rotation matrix error in Frobenius norm

the peaks corresponding to frequencies $-\psi$ and $-\varphi - \psi$. For $\tau = 4s$, the peaks corresponding to $-\psi$ are perturbed by side oscillations of the main lobe. The estimation becomes less accurate.

6. CONCLUSION

In this paper, we have demonstrated that the 3D rotation of a satellite in free motion can be estimated by means of embedded Sun sensors (illumination sensors) mounted on its surface. Some assumptions guaranteeing the non ambiguity of the measurements have been established by a careful study of the solutions of the free rotation dynamics and have been formulated in terms of its inertia parameters, its angular momentum, and its initial nutation.

The problem under study in this contribution is relatively general. Specific studies could be conducted in a similar manner for other governing dynamics: for spinning missiles or ammunitions in atmospheric flight, or other sorts of projectiles. Interestingly, one could draw some parallel between our application and some recent works. In a completely different area, Kitani et al. [2012] consider a camera being embedded in an American football, in

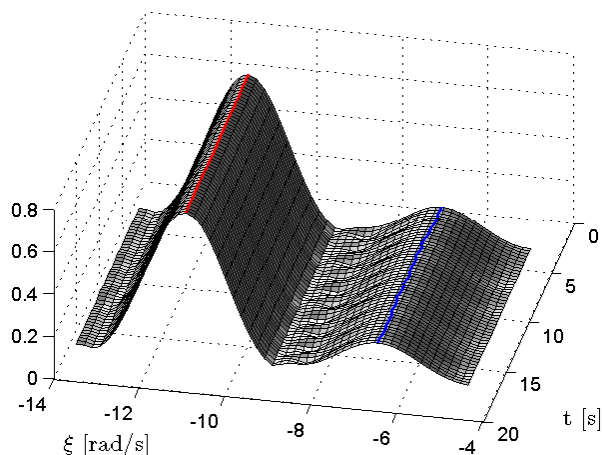


Fig. 6. Spectrogram for $\tau = 6$ s

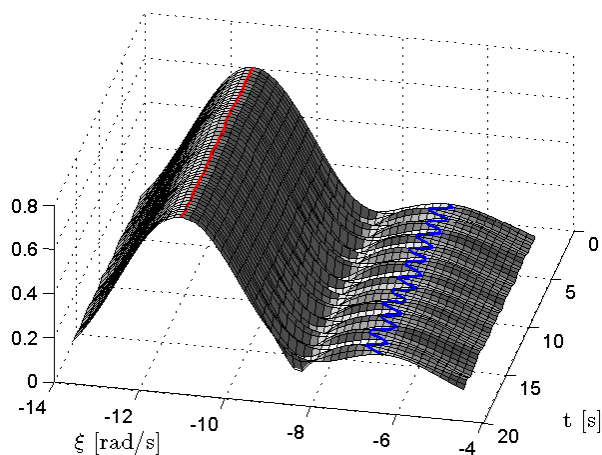


Fig. 7. Spectrogram for $\tau = 4$ s

order to provide the spectator of the game a third-person point-of-view (the ball's viewpoint). In this application, estimating the camera rotation is a prerequisite to cancel the extreme spinning motion of the camera during flight, in view of aligning the frames in the video by subsampling of the recorded sequence. Our approach could probably be used to provide a continuous estimate of the rotation, in 3D, for improved video reconstruction.

Other paths for future research could also concern a dual problem where the sensors are not embedded but remote and fixed (Hewgill [1992]). The cameras would then be used to reconstruct the 3D rotation of the rigid body. This problem is of importance in numerous autonomous robotics applications. For example, in the aerospace area, it is often desired to grasp a tumbling object, or a satellite. The tumbling motion is usually generated by a malfunctioning of the satellite attitude control system, which eventually gives rise to a free rotation motion. Capturing of such object has been in the scope of numerous on-orbit servicing project (see e.g. Landzettel et al. [2006]) where rotation estimation is a critical issue. We believe that illumination sensors employed with an algorithm similar

to the one presented in this article could be a relevant technique in this context.

REFERENCES

- Abraham, R. and Marsden, J. (1978). Foundations of mechanics. Addison Wesley, 2nd edition.
- Abramowitz, M. and Stegun, I.A. (eds.) (1964). Handbook of mathematical functions with formulas, graphs and mathematical tables. Dover Publications.
- Bak, T. (1999). Spacecraft attitude determination - a magnetometer approach. Ph.D. thesis, Aalborg University.
- Bruninga, B. (2007). Determining the attitude and rotation rate of atmospheric neutral density experiment. Technical report, US Naval Academy Satellite Lab.
- Choukroun, D., Bar-Itzhack, I.Y., and Os (2006). Novel quaternion Kalman filter. IEEE Transactions on Aerospace and, 42(1), 174–190.
- Hall, J.M. and Harris, M. (1970). Spacecraft Sun sensors. Technical report, NASA.
- Hewgill, L. (1992). Motion estimation of a freely rotating rigid body in earth orbit. In SPIE Cooperative Intelligent Robotics in Space III Proceedings, volume 1829, 444–457.
- Kitani, K.M., Horita, K., and Hideki, K. (2012). Ballcam! Dynamic view synthesis from spinning cameras. In ACM Symposium on user interface software and technology (UIST).
- Landau, L. and Lifchitz, E. (1982). Mechanics. MIR Moscow, 4th edition.
- Landzettel, K., Preusche, C., Albu-Schaffer, A., Reintsema, D., Rebele, D., and Hirzinger, G. (2006). Robotic on-orbit servicing - DLR's experience and perspective. In IEEE/RSJ International conference on intelligent robots and systems.
- Magnis, L. and Petit, N. (2013). Rotation estimation for a satellite from Sun sensors. In European Control Conference (ECC), 852–859.
- Mallat, S. (1998). A wavelet tour of signal processing. Academic Press, San Diego, 1st edition.
- Murray, R.M., Li, Z., and Sastry, S. (1994). A mathematical introduction to robotic manipulation. CRC Press.
- Schmidt, M., Ravandoor, K., Kurz, O., Busch, S., and Schilling, K. (2008). Attitude determination for the Pico-Satellite UWE-2. In Proceedings of the 17th IFAC World Congress.
- Theil, S., Appel, P., and Schleicher, A. (2003). Low cost, good accuracy - attitude determination using magnetometer and simple sun sensor. In 17th Annual AIAA.USU Conference on Small Satellites.
- Wahba, G. (1965). Problem 65-1: a least squares estimate of spacecraft attitude. In SIAM Review, volume 7, 409.